Review Forma, **18**, 197–219, 2003

Complexity of Hydrodynamic Phenomena Induced by Spiral Waves in the Belousov-Zhabotinsky Reaction

Hidetoshi MIIKE[1]* and Tatsunari SAKURAI[2]

[1]*Department of Perceptual Sciences and Design Engineering, Yamaguchi University,*
Tokiwadai 2-16-1, Ube 755-8611, Japan
[2]*Department of Electrical Engineering, Ube National College of Technology,*
Tokiwadai 2-14-1, Ube 755-8555, Japan
**E-mail address: miike@kde.yamaguchi-u.ac.jp*

(Received August 18, 2003; Accepted November 17, 2003)

Keywords: Belousov-Zhabotinsky Reaction, Reaction-Diffusion-Convection System, Marangoni Effect

Abstract. We review a series of experimental investigations on the oscillatory hydrodynamic flow appearing in a thin solution layer of the Belousov-Zhabotinsky (BZ) reaction under excitation of spiral waves. There have been many investigations to clarify the mechanism of the flow. Starting from a historical sketch, we introduce the latest findings, those closely relate to the mechanism of the oscillatory flow. In discussion and remarks, we summarize curious characteristics of the oscillatory flow and discuss the mechanisms establishing the flow to draw out a picture for the better understanding of the phenomena. Utilizing the hydrodynamic flow induced by the chemical spiral waves themselves, the chemical waves seem to maintain their original reaction-diffusion structure in the batch reactor. This can be regarded as a function of the system.

1. Introduction

Spiral waves are known as representative structures in dissipative systems observed in a reaction diffusion system such as the Belousov-Zhabotinsky (BZ) reaction (VIDAL and HANUSSE, 1986; WINFREE, 1987). Self organization is observed as a spatial and temporal structure of chemical activity in a non-stirred batch reactor containing the BZ-solution (see Fig. 1). The occurrence of traveling chemical waves in this system, such as target patterns (see Fig. 1(a)) or rotating spirals (see Figs. 1(b), (c) and (d)), has been treated theoretically by modeling the nonlinear chemical reaction kinetics coupled with molecular diffusion (VIDAL and HANUSSE, 1986; WINFREE, 1987; KAPRAL and SHOWALTER, 1995). A lot of numerical investigations on the reaction-diffusion systems have brought fruitful results that help to understand the system. Self-replicative patterns (PEARSON, 1993), meandering spirals (JAHNKE and WINFREE, 1991; LEE *et al*., 1994; MIKHAILOV *et al*., 1994; ITO, 1994), and stationary structures of the Turing patterns (TURING, 1952; CASTERS *et al*., 1990) are these representatives as well. Experimentally, an ideal system for these reaction-diffusion

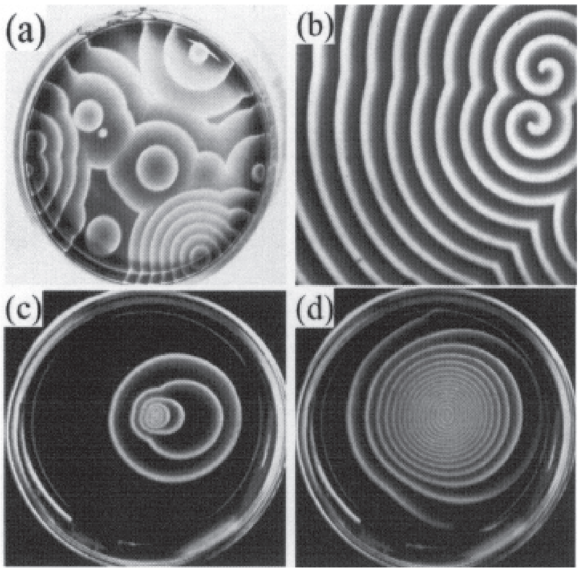

Fig. 1. Chemical waves in a thin solution layer (about 1 mm depth) having liquid/gas free interface in the Belousov-Zhabotinsky reaction. (a) Spontaneous excitation of chemical waves. Many target patterns are easily excited spontaneously in the uncontrolled Petri dish. Careful treatment of the solution and patient maintenance of the dish may realize the condition of no spontaneous excitation of the waves and no CO_2 bubble nucleation (see text and compare to (b), (c) and (d)). (b) Rotating chemical spiral waves having a twin rotor. (c) and (d) Development of the rotating spiral pattern. The wavelength of the pattern decreases with time. The minimum wavelength is about 1 mm and the period of spiral rotation is about 18 s.

models has been pursued. One of the solutions is a gel system with combination of continuously fed unstirred open reactors or continuous flow unstirred open reactors (CFURS) (NOSZTICZIUS *et al.*, 1987; TAM *et al.*, 1988; CASTERS *et al.*, 1990; DE KEPPER *et al.*, 1991; KSHIRSAFER *et al.*, 1991). Convection associated with the chemical reaction can be suppressed in the gel system. The discovery of the Turing structures in the chlorite-iodide-malonic acid (CIMA) reaction was realized by use of the gel system (CASTERS *et al.*, 1990; DE KEPPER *et al.*, 1991).

On the other hand, hydrodynamic phenomena induced by chemical reaction play important roles to realize self organizing complex systems. Convection driven by density (Rayleigh-Bénard type) or by surface tension (Marangoni type) coupled with chemical reaction has brought curious phenomena in reaction-diffusion systems. These systems can be treated theoretically by modeling reaction, diffusion and convection, which may bring a plenty of possible pattern dynamics such as spatio-temporal chaos, functional order, and more hierarchical and complex pattern dynamics (FIELD and BURGER, 1985; WU *et al.*, 1995; DIEWALD and BRAND, 1995). In this paper we review hydrodynamic phenomena associated with rotating spiral waves in the BZ reaction. The following sections contain historical sketch, experimental aspect, theoretical approaches, recent developments, and discussion and remarks.

2. Experimental and Historical Sketch

2.1. Experimental setup

Experiments were carried out in an excitable BZ-solution catalyzed by ferroin in a batch reactor (Petri dish, diameter 6.8 cm) at room temperature 25°C (MIIKE *et al.*, 1988a). The BZ reaction was obtained by preparing a mixture of 48 mM sodium bromide, 340 mM sodium bromate, 95 mM malonic acid, and 378 mM sulfuric acid. About 5 min after mixing, the catalyst and indicator ferroin (3.5 mM) was added. All solutions were filtered through Millipore filter (0.22 μm). Subsequently polystyrene particles (0.48 μm) serving as scattering centers were mixed into the solution. With the small amount (about 10^6 particles/ml) of polystyrene used no effect on the pattern evolution was confirmed. The mixture was filled into a Petri dish to a depth of 0.85 (±0.5) mm. Experiments were carried out with or without covering the dish with a glass plate. The procedure for triggering spiral waves is introduced in reference (MüLLER *et al.*, 1987). An air gap of about 12 mm was left between the layer surface and the glass cover. Fresh samples were prepared for each experiment. The experiments were started ($t = 0$) soon after triggering the spiral waves in the solution.

It should be noted that all the above mentioned phenomena of hydrodynamic instability are observed only under a "clean" condition. The clean condition requires:

a) distilled and ion-exchanged pure water in the preparation of BZ reagents,
b) scratch-free and dust-free Petri dish, and a clean room for the experiments, and
c) careful treatment and patient maintenance of the inner surface of the Petri dish.

Ideally speaking, the Petri dish should be kept under the flow of the pure water.
Under these conditions, spontaneous excitation of chemical waves and nucleation of CO_2 bubble are almost suppressed. We can distinguish the BZ patterns under these conditions from those under the ordinary conditions with uncontrolled contamination and/or dust (see Fig. 1(a)). Only controlled chemical waves with desirable location of the center of spiral structure are allowed for the present experiments. A typical example of the well-controlled spiral waves is shown in Figs. 1(c) and (d).

Observation of chemical activity and hydrodynamic phenomena were carried out by microscope video imaging system (MÜLLER *et al.*, 1985b). To visualize hydrodynamic flow in the BZ-solution, laser light illumination and polystyrene particles as scattering centers were introduced. The system comprised of a He-Ne laser (632.8 nm), an inverted microscope, a TV-camera, a video recorder and a personal computer. A schematic is given in Fig. 2. The key point of the technique is the simultaneous illumination by laser light focused to an area with diameter of about 0.2 mm and homogeneously transmitted monochromatic light field using an interference band-pass filter of 480 and the selected optical wavelength corresponds to the maximum difference between the absorption of oxidized and reduced form of the catalyst. The monochromatic transmitted light visualize propagating waves of chemical activity. Particles illuminated by the laser light allow to measure the hydrodynamic flow. We usually focus into a plane close to the surface of the solution layer. In this system, the layer depth can be measured with good precision (±0.05 mm) by changing the focus of the observation plane of the microscope. Figures 2(a) and (b) show examples of the image sequence observed by the microscope. Motion of the polystyrene particles is well visualized by laser light illumination. Temporal trace of

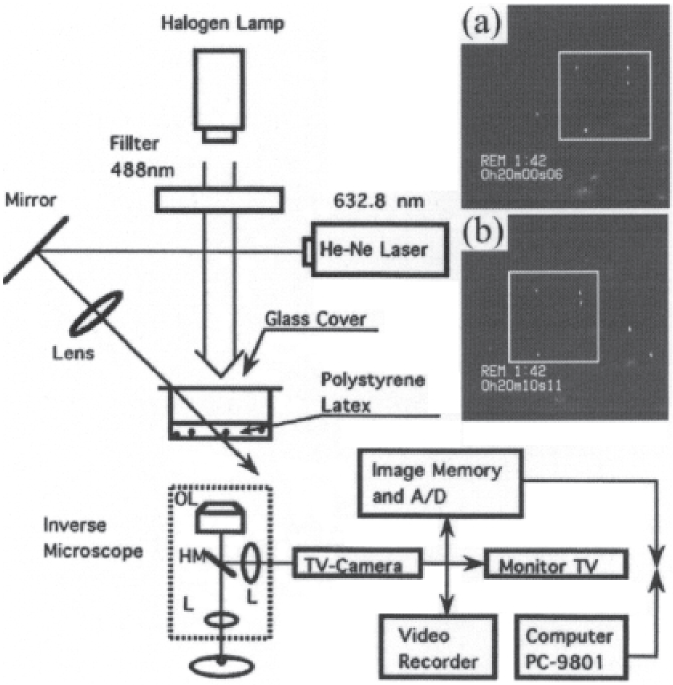

Fig. 2. A schematic diagram of the microscope video imaging system. Simultaneous measurement of chemical activity and hydrodynamic motion is realized. (a) and (b) Motion of polystyrene particles during 10 s under the inverted microscope. The particles are illuminated by a He-Ne laser light to trace the hydrodynamic motion.

velocity is analyzed automatically in every one second by spatial filtering velocimetry based on the image sequence processing (MIIKE *et al.*, 1997).

2.2. *Convection associated with chemical waves*

In this chapter we present a historical sketch (before 1995) of the oscillatory hydrodynamic flow observed in the BZ-solution layer. Considering an analogy to the Turing instability (TURING, 1952) in biological systems, many researchers tried to find out stationary dissipative structures in chemical systems such as the BZ-solution (BORCKMANS and DEWEL, 1988). Interactions between propagating chemical waves and stationary convection cells was considered as such examples (ORBAN, 1980; AGLADZE *et al.*, 1984; MÜLLER *et al.*, 1989). Only evaporative cooling of the solution surface induces convection under open free interface. This type of convection is attributed to the Marangoni instability (SCHWABE *et al.*, 1992). Figure 3 shows one example. A static pattern of the convection roll appears within 3 minutes after removing the cover of the Petri dish. The convection pattern (a "mosaic" pattern) itself is not unusual. MÜLLER *et al.* (1985a) reported examples of the surface tension driven convection in chemical and biochemical systems. In these systems,

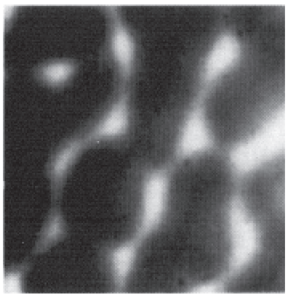

Fig. 3. A “mosaic” convection pattern appeared in the BZ solution layer under uncovered liquid/gas interface (MIIKE *et al.*, 1988a).

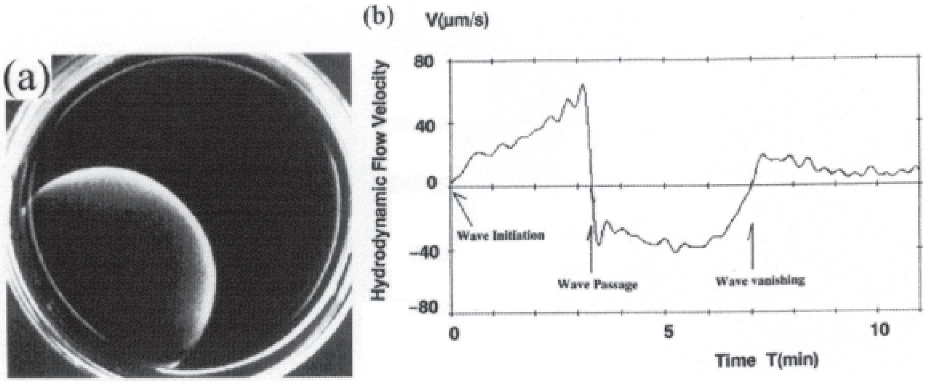

Fig. 4. (a) Excitation of a single chemical wave which propagates with a constant velocity v. The size of the dish is about 6.8 cm. (b) Hydrodynamic flow induced by the single circular wave propagation. The velocity of the flow v_s is measured near the surface of the BZ solution layer. Direction of the flow measured near the surface is reverse to that of the flow measured near the bottom.

however, the chemical reaction merely serves to visualize pre-existing hydrodynamic currents (BORCKMANS and DEWEL, 1988). The convection pattern is suppressed by covering on the top of the dish to prevent the evaporation.

We often observe many spontaneous excitations of target patterns and/or spiral waves in a Petri dish under a usual situation of the experiment (see Fig. 1(a)). Uncontrolled chemical activities create accidental patterns of chemical waves. Under these incoherent conditions of chemical waves, it is hard to observe coherent pattern dynamics of hydrodynamic flow. Careful treatment of materials and sufficient control of experimental conditions bring a quite different physical condition for the non-linear pattern dynamics (Fig. 1). Intrinsic phenomenon of convection caused by chemical waves itself was first found with the oscillatory hydrodynamic flow in spiral waves during the BZ reaction just

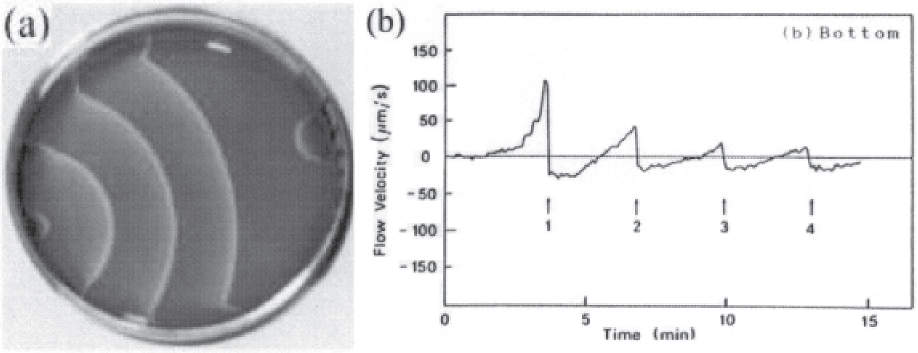

Fig. 5. (a) Periodic initiation of circular waves in a BZ solution layer (MIIKE *et al.*, 1989). (b) Time trace of the flow velocity measured near the bottom $v_b(t)$ of the circular waves in the BZ solution layer (MIIKE *et al.*, 1989). The direction of chemical wave coincides with that of positive flow velocity.

only under an open liquid/gas interface in a batch reactor by MIIKE *et al.* (1988a). They suggested that the oscillatory flow is induced by the coupling between chemical waves and surface tension-driven convection. Here we survey the hydrodynamic phenomena directly induced by chemical waves under the condition to prevent evaporation.

2.3. Convection traveling with circular waves

A simple experiment with preventing the evaporation from layer surface was carried out to investigate the mechanism of the oscillatory flow associated with spiral waves (MIIKE *et al.*, 1989). The simplest limit is an excitation of a single circular wave. Hydrodynamic flow velocity was measured at the surface of a BZ-solution layer with a single circular wave as shown in Fig. 4. The flow direction was towards the wavefront of the wave approaching the observation area. We defined this direction to be positive. The surface flow velocity v_s changes its direction suddenly after the passage of the chemical wave. After vanishing of the wave at the end of the dish, the flow changes its direction again and decreases its amplitude with time.

Figure 5 shows the hydrodynamic motion induced by a target pattern. When the wavelength between circular waves is large enough (let us say 10 mm), passage of each circular wave induces a hydrodynamic motion. There occurs a directional flow near the solution surface. The flow first points towards the wave front and increases the velocity as the front approaches the fixed observation area. After wave passage, the surface flow suddenly reverses its direction. By contrast, the direction of hydrodynamic flow near the bottom v_b shows the opposite behavior as shown in Fig. 5. Sign of the velocity is of Fig. 4.

The results of the discrete waves experiments (including the single chemical wave), can be summarized as follows:

1) a chemical wave can induce a convection,

2) the convection rolls propagate with chemical waves in the thin (<1 mm) BZ-solution layer.

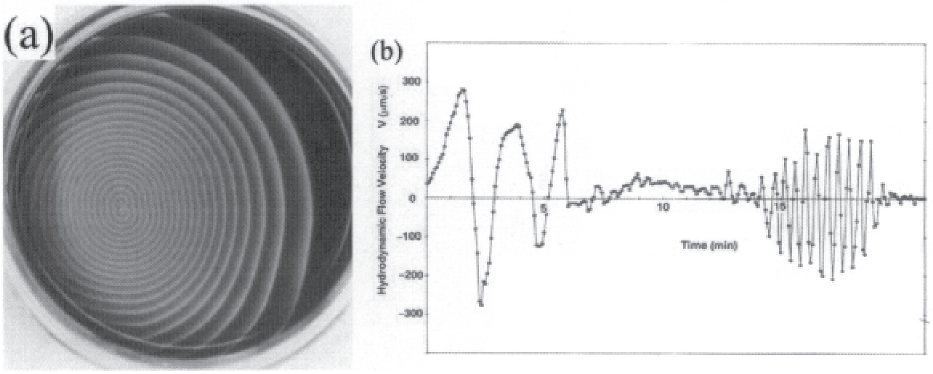

Fig. 6. (a) Chemical spiral waves with 1 mm wavelength. (b) Time trace of the hydrodynamic flow v_s measured locally near the surface of the BZ solution. In the early stage, pronounced amplitude of the flow velocity was observed. The flow was associated with the discrete chemical waves excited initially. Flow oscillation began at around 15 min after triggering the waves when the spiral was well developed.

2.4. From discrete waves to dense wave trains (oscillatory flow associated with spiral chemical waves)

When we trigger a spiral wave pattern, the wavelength of the wave trains tends to decrease with time (see Figs. 1(c), 1(d) and 6(a)). The minimum wavelength is about 1 mm at around 7 min after triggering the spiral waves. In this condition of dense wave trains, recovering time of the chemical system back to the reduced state is not enough after passage of the waves. Judging from the light absorption, concentration change of $[\mathrm{Fe(phen)_3}]^{3+}$ at the wave front becomes small with time. Then, as mentioned in the following section (Sec. 4), each wave may lose an ability to induce convection (see Fig. 5(b)). Concentration gradient of $[\mathrm{Fe(phen)_3}]^{3+}$ contributes to brings surface tension gradient.

Figure 6 shows a continuous change of the hydrodynamic flow from discrete sparse waves to dense waves. At the beginning, when the first wave was approaching the observation area, the flow direction was towards the wavefront. The flow direction suddenly changed at the passage of the waves. These waves propagated into a relatively well-reduced medium; therefore, the behavior of the convective flow was similar to that of the flow induced by a single circular wave as shown in Figs. 4 and 5. The first and the second waves, however, induce big amplitude (about v_s = 300 μm/s) of hydrodynamic flow velocity. Under well-controlled conditions, these waves show curious characteristics of accelerating velocity of wave propagation. The wave is called "Big Wave" (MIIKE *et al.*, 1992, 1993; KAI *et al.*, 1995). Mechanism of the acceleration is not well understood yet. However, we will not proceed into the details of this problem in this report. In the second stage, the distance between the wavefronts of the spiral waves decreased from 10 mm to 1 mm as ten or more waves passed the observation area. Because the spiral wave train propagated into a less reduced medium than the first stage due to the short wavelength, the velocity of the induced flow decreased with time. In this stage, there was no correlation between the chemical wave passage and the flow direction. Only a small amplitude of mean flow appeared until the oscillatory flow begins. The direction of the flow near the surface was toward the center of spirals. After 14 min, however, the flow suddenly started to oscillate with a large amplitude of flow velocity, up to 100 μm/s, and the oscillation continued for several minutes (the third stage). In this stage, the flow direction changed synchronously with each passage of the chemical waves. That means the period of the flow, called oscillatory flow, was almost twice as large as that of the passage of the chemical waves, which suggests a possibility of a period doubling entrainment of hydrodynamic flow by chemical wave trains.

Successive experimental investigations (MIIKE *et al*., 1988b, 1989; MÜLLER and MIIKE, 1990; MIIKE and MÜLLER, 1993) indicated important findings on the oscillatory flow. These are:

1) oscillatory deformation of chemical waves induced by the flow oscillation (MIIKE *et al*., 1988b),

2) period-doubling behavior of the oscillatory deformation suggesting entrainment of flow oscillation by periodic passage of chemical wave trains (MIIKE *et al*., 1988b),

3) observation of the oscillatory flow even under such conditions as covered with glass plate leaving an air gap of about 12 mm (MIIKE *et al*., 1989), and

4) chaotic decomposition of spiral waves by the fully developed oscillatory flow (MIIKE and MÜLLER, 1993).

All of the above experiments were carried out in a Petri dish. Only one twin rotor of spiral waves is recognized at the center of the pattern (compare with the uncontrolled dish in Fig. 1(a)).

3. Theoretical and Numerical Approaches

3.1. Density driven convection

First trial of numerical analysis was made by PLESSER *et al*. (1992) to explain the convection induced by chemical waves. They clarified that the assumption of density differences between the bulk of the solution and the waves is sufficient for an explanation of the convection. The exothermicity of the reaction and the differences in partial molar volumes between products and reactants can always cause a density gradient (POJMAN and EPSTEIN, 1990; POJMAN *et al*., 1991a, b). However, their approach was a time-independent model of the reaction-diffusion-convection interaction for an interpretation of the experiment on circular waves propagation (see Figs. 4 to 5). They also suggested the importance of the combined time-dependent effects of both the density driven convection in the bulk and the thermocapillary forces at the boundary. DIEWALD and BRAND (1993) proposed a simple model for chemically driven convection. They presented a qualitative discussion on the relationship between their envelope equation and the experimental results. They also referred to the 1:2 relation between passage of chemical wave fronts and the reversal of the flow direction at a certain point (MIIKE *et al*., 1988a). They assumed that the density gradient is due to the concentration variations in the reaction-diffusion patterns driving the convection.

3.2. Surface tension driven convection

On the other hand, YOSHIKAWA *et al*. (1993) found a direct evidence of thermocapillary

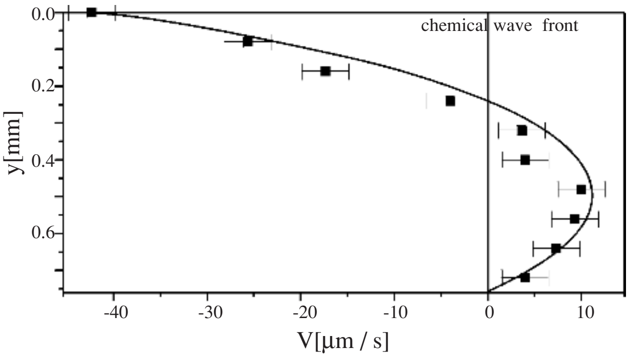

Fig. 7. Comparison between experiments (rectangles with error bar) and simulation (curve) with the velocity profile $v(y)$ of convection induced by a single chemical wave (MATTHIESSEN *et al.*, 1996). On the courtesy of Prof. S. C. Müller.

forces of the chemical reaction by measuring periodic change of the surface tension in a continuously stirred BZ reaction. They suggested that the difference in surface tension between the two states of the iron-catalyst $[Fe(phen)_3]^{3+}$ and $[Fe(phen)_3]^{2+}$ was the driving force of the rhythmic phenomenon. Thus, concentration gradients of iron-catalyst at the wave front can be a driving force of the convective flow. First quantitative explanation for the convective flow associated with chemical waves was proposed by MATTHIESSEN *et al.* (1996). The mechanism of the chemically driven convection was investigated with space-resolved velocimetry using a set-up similar to Fig. 2, and simulated numerically by solving a set of modified Oregonator model equations and the Navier-Stokes equation (see Appendix A.1). The result of a surface tension flow matches best to experimental findings (see Fig. 7). MATTHIESSEN *et al.* (1996) suggested as follows: *The hydrodynamic flow generation is linked to the concentration of a chemical component that shows a temporal evolution like the inhibitor. In the Oregonator model the inhibitor represents the concentration of the oxidized catalyst,* $[Fe(phen)_3]^{3+}$*. That is in a good agreement to the suggestion of Yoshikawa et al. (1993) (see preceding paragraph) that the* $[Fe(phen)_3]^{3+}$ *concentration difference is the cause of the surface tension gradient in the BZ reaction.* The surface tension gradients induce a convection, which is known as the Marangoni-type convection or thermocapirally convection (see Appendix A.2). Thus, it was clarified that the surface tension driven convection caused by the solutal Marangoni instability plays a major role to induce flows associated with the discrete circular waves propagating in the BZ solution.

As is well known, the surface tension is also affected by thermal changes. Recent investigation clarified that an exothermic reaction in the chemical wave front generates a local temperature rise of 50 mK (BÖCKMANN *et al.*, 1996). They conclude that the direction of the change allows to exclude the possibility of the contribution of thermal Marangoni mechanism. A clue is obtained to understand the chemically driven convection. However, this is only a first step to uncover the mechanism of the flow oscillation induced by spiral waves.

4. Recent Developments

4.1. Flow waves

Recently, we have had several important findings to understand the oscillatory flow associated with rotating spiral waves in the BZ reaction. These findings are:

1) global flow waves in chemically induced convection (MATTHIESSEN and MÜLLER, 1995),

2) propagation of surface deformation coupled with the convection waves (SAKURAI *et al*., 1997a),

3) initiation front and annihilation center of convection waves developing in chemical spiral patterns having two spiral centers (SAKURAI *et al*., 1997b), and

4) dish size dependent characteristics of the propagation velocity of the convection waves (SAKURAI *et al*., private communication, 2000).

MATTHIESSEN and MÜLLER (1995) investigated a global structure of the flow oscillation.

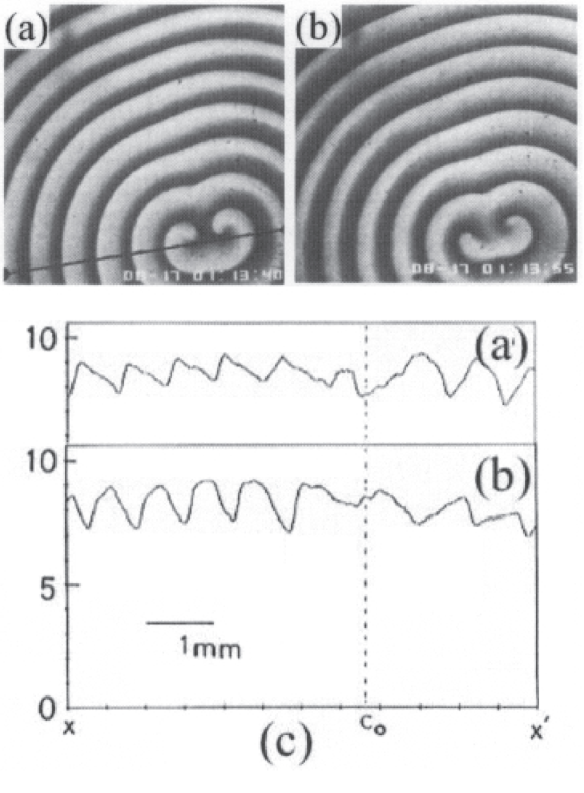

Fig. 8. Deformation of chemical wave profiles by the oscillatory flow (MIIKE and MÜLLER, 1993). Sectional profiles along tilted solid line in (a) are shown in (c). Left half profiles in (c) are with surface flow against (a) and in the direction (b) of wave propagation. On the courtesy of Prof. S. C. Müller.

They found large flow waves with a wavelength on the order of ten chemical wavelengths traveling through the dish towards the center of the underlying spiral waves. To visualize a global distribution of the flow direction, they utilized the deformation of chemical wave profiles modified by hydrodynamic flow. The concentration profile of a chemical wave traveling against the direction of surface flow differs slightly from that traveling in the direction of the flow (see Fig. 8). Image processing enhances the slight difference on brightness. The result of the processing is shown in Fig. 9, in which the spiral center is placed at the middle of the dish. They reported as follows: *A bright band appears in the second image (b) with a circular geometry near the dish boundary. It moves towards the spiral center as time proceeds and finally disappears. The bright band represents surface flow in the direction of wave propagation. As the bright bands show regions with simultaneously tilted wave fronts we observe a large global flow wave traveling through the dish towards the spiral center.* They also suggested that possible driving forces are gradients in the local density or surface tension induced by difference in the composition of the solution.

Stimulated by the above novel findings, both experimental and numerical studies were encouraged. DIEWALD and BRAND (1993) and DIEWALD *et al.* (1996) carried out analytical

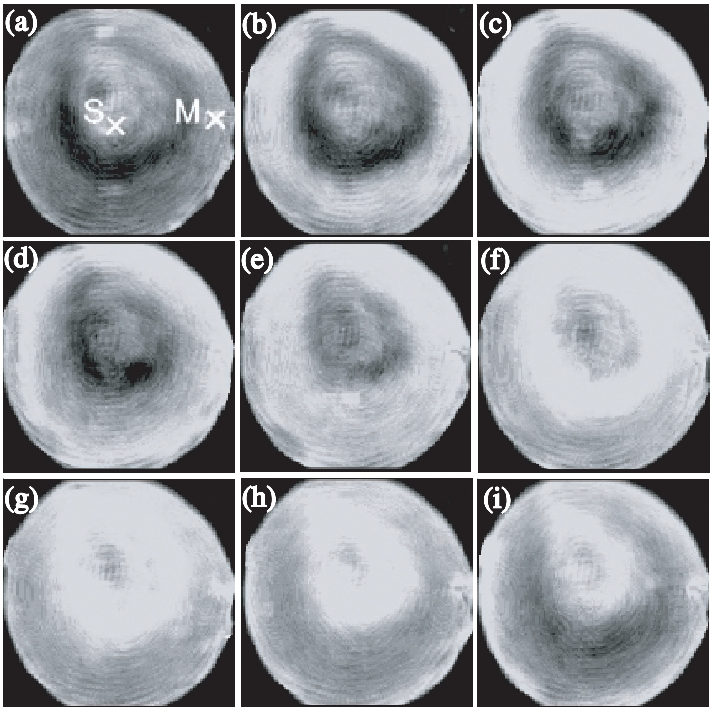

Fig. 9. Global view of the oscillatory flow. The center of the spiral structure (s) is in the middle of the dish (MATTHIESSEN and MÜLLER, 1995). The propagating structure (flow waves) has the velocity v_f about 0.5 mm/s).

and numerical approaches on chemically driven convection. In particular, DIEWALD *et al.* (1996) discussed how a group of chemical waves drives an oscillatory convective motion in a fluid layer by use of a two species reaction-diffusion model coupled with the hydrodynamic equation. The mechanism considered is a variation of the surface tension along a free surface due to an inhomogeneous concentration distribution. Their comments seem to hit an essential point of mechanism to induce flow waves (the oscillatory flow) in spiral waves.

4.2. Surface deformation waves

Accompanied with the flow waves a propagation of surface deformation was found by SAKURAI *et al.* (1997a). Figure 10 shows temporal traces of the surface tilt angle and that of surface flow velocity. The behavior of the surface tilt was synchronizing well with the flow oscillation. The surface deformation $h(t)$ can be evaluated from the local tilt angle $\beta(t)$ under the assumption of constant propagation velocity v_d of the deformation waves:

$$h(t) = \int_0^t v_d \tan \beta(t) dt, \tag{1}$$

where v_d was estimated to be 2.5 mm/s in the system as shown in Fig. 6(a) (the wavelength of the deformation waves is about 100 mm). The velocity v_d is about more than 25 times the velocity of chemical waves v. The estimated time trace of $h(t)$ is shown in Fig. 11. The maximum deformation $h_m(t)$ of the solution layer is about 2.0 μm, which is formed when the flow velocity v_s becomes zero. Phase shift between v_s and $h(t)$ is $\pi/2$. The velocity of deformation wave v_d is coincident with that of flow waves v_f. Note that the observed velocity of flow waves by SAKURAI *et al.* (1997a) is almost 5 times faster than that by MATTHIESSEN and MÜLLER (1995). This is most likely caused by the difference of

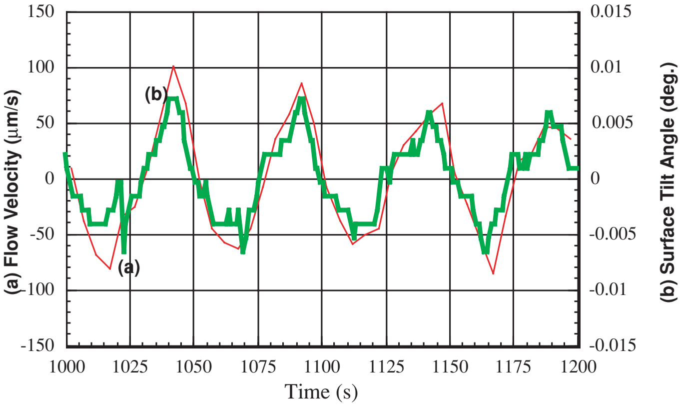

Fig. 10. Comparison of temporal traces between the surface flow velocity v_s (thin line) and the local tilt angle β of the solution surface (thick line). The oscillation period T is about 40 s at 25°C, which is almost twice as the rotation period of the spiral waves (about 20 s) (SAKURAI *et al.*, 1997a).

observed temperature of the BZ-solutions between two laboratories. Observed temperature was 16°C (MATTHIESSEN and MÜLLER (1995)) and 25°C (SAKURAI *et al.* (1997a)), respectively.

Taking above experimental results into account, SAKURAI *et al.* (1997a) concluded a picture as shown in Fig. 12. The global structure of convection roll having a periodic surface deformation propagates through the edge of the dish towards the spiral center as illustrated in the figure. This is a possible scheme to explain the oscillatory convection and the oscillatory surface deformation only together with a coupling between surface tension and chemistry as proposed in (MATTHIESSEN *et al.*, 1996) and here in Sec. 4. Sakurai *et al.* also suggested that: *the Marangoni convection, having a long-scale surface deformation caused by non-uniform surface tension associated with chemical waves development, may play a role in establishing these curious pattern dynamics observed in a reaction-diffusion-convection system.*

4.3. Switching flow waves

Recently, SAKURAI *et al.* (1997b) reported a novel switching structure of the flow waves. The experiment was carried out in a system as shown in Fig. 13(a). Two spiral structures are excited in the same solution layer of the BZ reaction. Each structure has a twin rotor of chemical waves. Two structures cause a collision line (a horizontal centerline in Fig. 13(a)) of chemical activity in the center of the dish. They found periodic initiation of moving structure of convection (flow waves) from the collision line (see Fig. 13(b)). The waves of convection propagated toward the respective center of spiral structure, and were annihilated there. In the system, the convection wave is emanating in alternate directions every 15–16 s (the period of oscillation T is about 30 s). The periodic pattern of chemical waves from the two-twin-rotors was modified by the running convection wave initiated from the collision front. The velocity of the wave v_f and its wavelength λ were 1.25 mm/

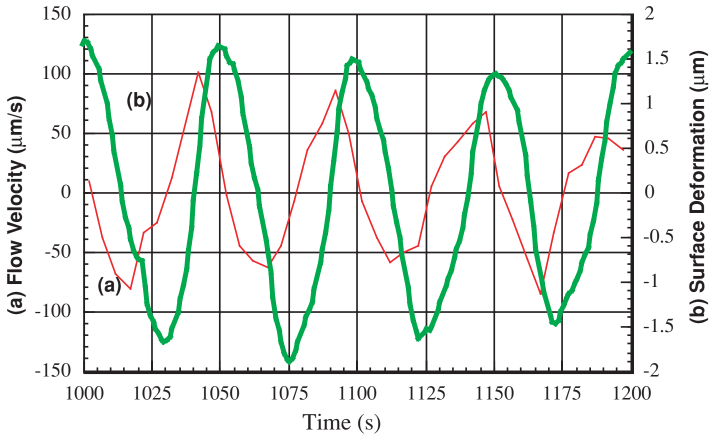

Fig. 11. Comparison between the convection velocity v_s (thin solid line) and the surface deformation $h(t)$ (thick solid line) obtained by Eq. (1) (SAKURAI *et al.*, 1997a).

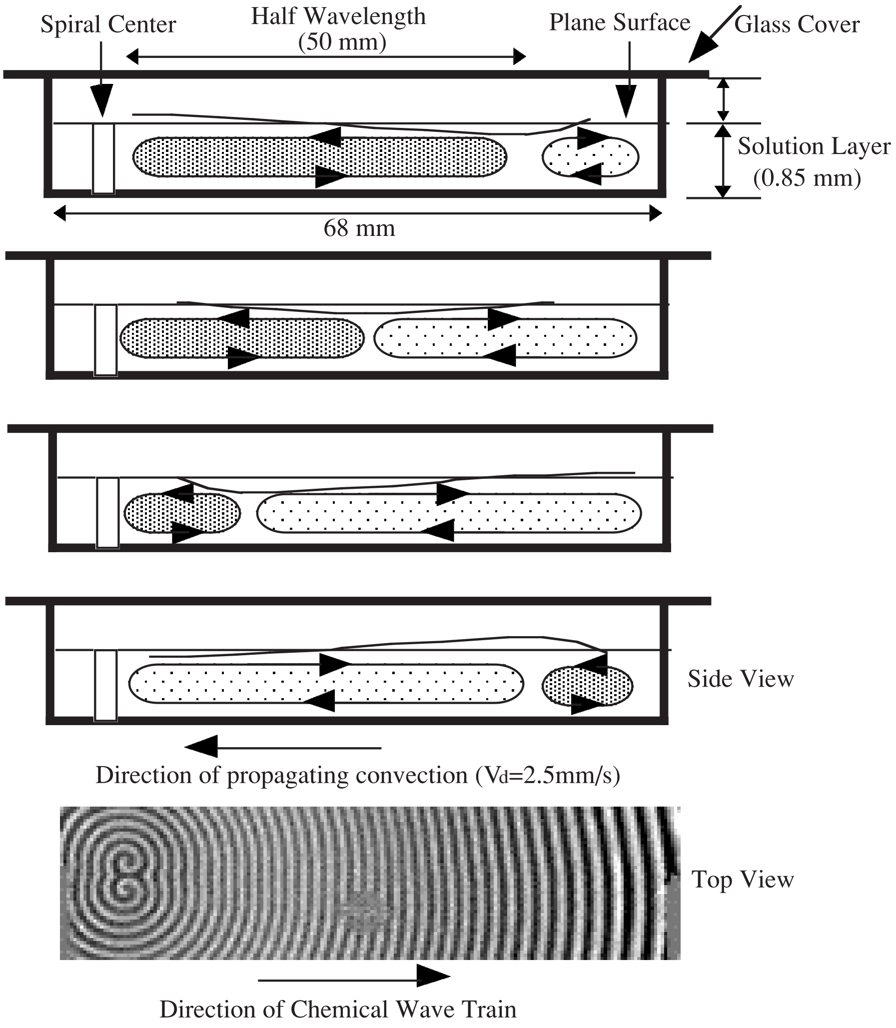

Fig. 12. A possible scheme to explain the oscillatory flow (SAKURAI *et al.*, 1997a). The convection waves (flow waves) having a long wavelength with a long scale surface deformation propagates from the edge of the dish towards the center of the spiral structure. The wavelength λ and the velocity of deformation waves v_d are about 100 mm and 2.5 mm/s, respectively.

s and 37.5 mm, respectively. Note that the well-known relationship is given by

$$v_f = \lambda/T. \tag{2}$$

In Fig. 13(b) the hydrodynamic flow oscillation v_s measured simultaneously is superimposed

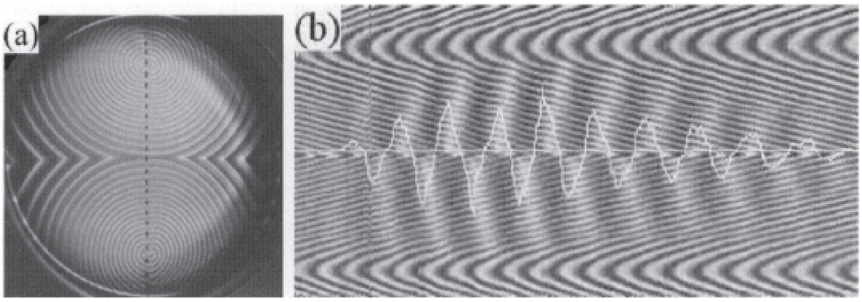

Fig. 13. (a) Collision of two spiral waves (SAKURAI *et al.*, 1997b). The two twin rotors are initiated at the same time and are located as mirror-symmetrical. (b) Space-time profile of the chemical activity along the vertical dotted line connecting two centers of spiral structures (see (a)). Temporal trace of the surface flow velocity v_s is superimposed as a white line. Synchronization between the oscillatory flow and the periodic pattern modification (faint and broad structures emerging from the collision front) is recognized.

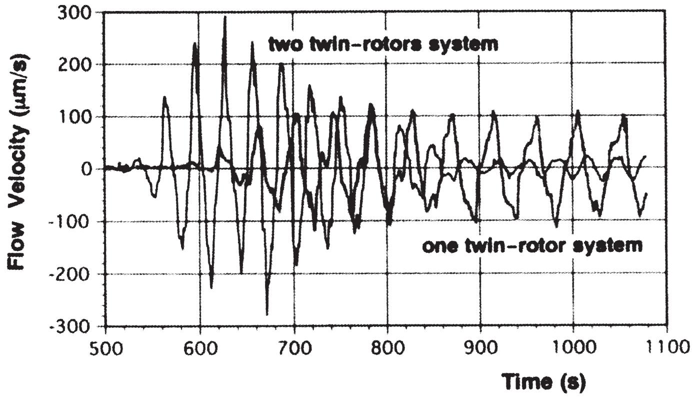

Fig. 14. Two examples of the oscillatory flow induced in the BZ solution layer under excitation of two types of spiral structures (SAKURAI *et al.*, 1997b). The black solid line shows flow oscillation v_s induced in a two-twin-rotors system (see Fig. 13). The grey solid line shows flow oscillation v_s induced in a one-twin-rotor system (see Fig. 6).

with a white solid line. The flow oscillation is synchronizing well with the switching pattern of the convection waves. Compared to the one twin-rotor system (see Fig. 6(a)), the two-twin-rotors system induces the oscillatory flow with enhanced amplitude, a shorter period and early induction time (see Fig. 14). The above results can be summarized:

1) the collision line of two chemical wave trains represents an origin for the waves of convection,

2) the running convection waves are initiated in alternate directions every 15–16 s, and

3) the respective centers of a spiral structure act as annihilation centers for the convection waves.

Namely, the twin rotor seems to develop into a sink area of the convection waves.

5. Discussion and Remarks

5.1. Summary of recent studies

In this paper, we have traced the history of study on the oscillatory flow induced in the BZ-solution layer under excitation of spiral waves. In the early stage of this study, the convection induced in the BZ-solution (reaction-diffusion system) was considered as only a kind of artifact. Evaporative cooling of the solution surface induces the Marangoni convection even in a shallow layer of the BZ reaction under open air/liquid interface. To realize an ideal reaction-diffusion system, gel systems were introduced to suppress the convection. Thus, the main stream of the study on non-linear dynamics in the reaction-diffusion system aimed to realize the open reactor serving as the ideal reaction-diffusion system (BORCKMANS and DEWEL, 1988).

In spite of this main stream, novel pattern dynamics have been found in a reaction-diffusion-convection system. These are

1) temporal oscillation of hydrodynamic flow induced spontaneously in the BZ-solution under excitation of spiral waves (MIIKE *et al*., 1988a, 1988b, 1989; MIIKE and MÜLLER, 1993),

2) propagating convection associated with discrete circular waves (MIIKE *et al*., 1989), and

3) "Big Wave" having an accelerating velocity of propagation (MIIKE *et al*., 1992, 1993; KAI *et al*., 1994, 1995).

As discussed in the preceding sections, many experimental results have been reported on these topics. These can be summarized as follows.

1) A chemical wave itself has an ability to induce convection. The concentration gradients of the iron-catalyst ($[\mathrm{Fe(phen)_3}]^{3+}$ and $[\mathrm{Fe(phen)_3}]^{2+}$) at the front of the chemical wave are the candidate for the driving force of the convection.

2) A vertical velocity profile of the convection induced by the discrete waves (circular waves) was explained quantitatively by numerical simulation. It was clarified that surface tension gradients are more effective than a density gradient in this system of the BZ reaction. On the oscillatory flow, recent studies established important characteristics of the phenomena. These are:

1) The oscillatory flow has a global structure of propagating flow wave.

2) The flow waves are initiated at the boundary of the dish or colliding front of two spiral patterns. These move toward the center of spiral structure as time proceeds and finally disappear.

3) The flow waves accompany surface deformation waves synchronizing with the hydrodynamic flow oscillation.

4) Switching flow waves were found in the system with two spiral structures of line symmetry in the dish.

In the latest study, we still obtained new findings. First is a dynamic behavior of the surface deformation which was pictured out by a direct observation with the Mach-Zehnder interferometer. It was clarified that the amplitude, the induction time and the period of the oscillatory flow depend on the characteristics of the system such as number of spiral structures and size of a Petri dish. Second is an observation of outgoing flow waves from the center of chemical spiral waves (SAKURAI *et al*., 2003). The flow waves show a target structure and develop to a spiral structure having a long wavelength about several cm. These results brought a quite different picture of the oscillatory flow. In spite of these new findings, however, origins of the oscillatory flows have still not been resolved. A key mechanism connecting the chemical activity and the global flow waves is not clarified.

5.2. Discussion

We briefly discuss on the mechanism of the flow oscillation and the flow waves. In this report, we have clarified the existence of convection waves that become organized spontaneously after formation of a spiral structure in the layer of the BZ-solution. It takes about 10 min to start the oscillatory flow after triggering the spiral waves. As time passes by, the triggered wave trains propagate to the end of the dish. It takes about 6 min for the wave train to reach the other end. Except for the triggered wave trains, spontaneous excitation of chemical waves is suppressed during the propagation. Note that a large number of chemical oscillations has occurred at the center of spiral structure until the first wave reaches the boundary. In this sense the system develops into a non-homogeneous state with global concentration gradients in space and time. As correctly suggested by DIEWALD *et al*. (1996), a variation of the surface tension along a free surface due to an inhomogeneous concentration distribution plays an important role to start the oscillatory flow. By the excitation of the convection waves the system proceeds into a new stage. Once the global convection field is established, the system may acquire new characteristics such as rapid and effective energy consumption and higher stability of the established structure (chemical spiral structure in this case). Faster energy consumption in a more highly organized system is confirmed by comparison of amplitudes, frequencies and induction times of the flow oscillation in one twin-rotor system with that of two twin-rotors system (see Fig. 14). Through effective mass transport caused by the reversing waves of convection (see Fig. 13(b)) inhomogeneous distribution of substrates (such as malonic acid and bromomalonic acid) is relaxed. Toward the center of spiral waves, the substrates necessary for continuing the reaction are supplied from the circumference area by the convection. This mechanism seems to play an important role to stabilize the spiral structure in the batch reactor. Thus, the development of a spiral structure produces an order of higher quality on a different hierarchical level. Dynamic transportation and/or coupling between chemical activity and convective flows are highly self-organized. As a result, a coherent structure appears (see Fig. 13(b)). These characteristics can be regarded as a kind of the functional order.

5.3. Some evidence and remarks

The organization of convection waves enables the system to homogenize the distribution of chemical substances. Therefore, it is expected to recover a more homogenized state in which the oscillatory flow stops. The oscillatory flow may start again as time proceeds to develop non-uniform distribution of the substrates and/or the catalysts. Typical experimental evidence is shown in Fig. 15. After the first flow oscillation, the BZ-solution seems to recover the original shape of spiral structures with the help of the oscillatory mixing of

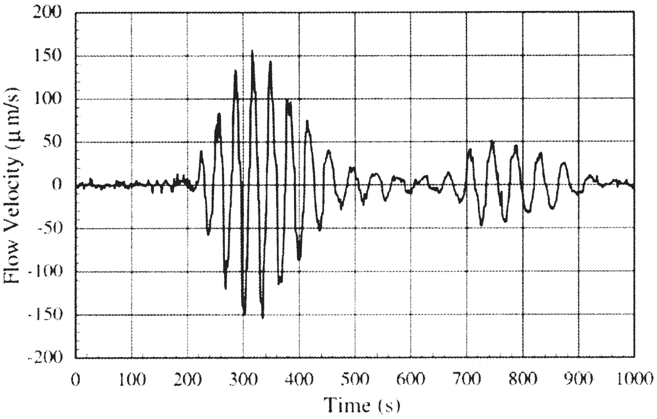

Fig. 15. Example of the repetition of hydrodynamic flow oscillation observed in the spiral waves during the BZ reaction.

convection. Induction of the convection feeds back the system to a more stabilized state. In this sense, the oscillatory convection can be regarded as a function of supplying substances from the circumference to the center of the spiral structure. This functional order helps the system to maintain the original dissipative structure. The above explanation, however, is no more than speculation.

The mechanism in which this hierarchical and functional order is established is not clarified yet. The Marangoni-type instability and associated long-scale surface deformation (SCHWABE *et al.*, 1992) may play important roles. Periodic deformation of the surface associated with the oscillatory flow should be taken into account. We have to emphasize the occurrence of non-uniform distribution of chemical species such as malonic acid, bromomalonic acid and the catalyst ferroin in the solution layer with development of the spiral structures. In particular, the strong surface activity of bromomalonic acid with curious dynamic behavior was found only recently by INOMOTO *et al.* (2000). Temporal decrease of the surface tension brought by bromomalonic acid production seems to explain the key mechanism of the Big Wave. They also measured local change of surface tension with the passage of chemical wave trains. They clarified that there are two types of temporal change in surface tension. One is a periodic sharp change associated with chemical waves. This is caused by the difference of the surface tension between $[Fe(phen)_3]^{3+}$ and $[Fe(phen)_3]^{2+}$ as discussed in Section 4. Therefore, the concentration gradient of the iron-catalyst at the front of a chemical wave can be the driving force of the convective flow associated with discrete chemical waves. The other change is a gradual decrease of surface tension with time. This curious phenomenon can be explained by a dynamic surface activity of bromomalonic acid (INOMOTO *et al.*, 2000). Existence of two surface tension activities, ferrin ($[Fe(phen)_3]^{3+}$) and bromomalonic acid, should be taken into account as a common mechanistic backgrounds to explain the Big Wave, solitary chemical wave (KAI and MIIKE, 1994; KAI *et al.*, 1995), and the oscillatory flow associated with spiral waves. Numerical approaches by modeling reaction, diffusion and convection with surface tension driven mechanism are encouraged.

We conclude that the development of the spiral waves induces a coherent structure of the flow waves and surface deformation waves, which is the cause of the oscillatory flow appeared in a thin solution layer of the BZ reaction. The structure can be interpreted as a demonstration of the hierarchical and/or functional order in a complicated system of reaction, diffusion and convection. Coupled with the convection waves the spiral waves seem to maintain their reaction-diffusion structure in the non-stirred batch reactor. In a finite open system, the energy source is consumed locally with time. Then, the system may induce a new order of convection structure to maintain the original reaction-diffusion structures in a different hierarchical level. This novel function may be regarded as a kind of primitive homeostasis, which is realized in the reaction, diffusion and convection system far from equilibrium.

Memorandum

Note that we have defined six different velocities of waves in the text. These are: v: velocity of chemical wave propagation, V: velocity of hydrodynamic flow, v_s: velocity of hydrodynamic flow measured near the surface of the dish, v_f: velocity of flow waves, v_d: velocity of surface deformation waves.

We thank Prof. S. C. Müller, Dr. E. Yokoyama, and Dr. A. Nomura for their helpful discussions and critical readings of the manuscript. It is also a pleasure to thank Dr. O. Inomoto, Dr. T. Yamaguchi, Prof. K. Yoshikawa and Prof. S. Kai for their stimulating discussions. This study was supported in part by a Grant-in-Aid for Scientific Research (B) (No. 15340125) and a Grant-in-Aid for Young Scientists (B) (No. 15740249) from The Ministry of Education, Culture, Sports, Science and Technology of Japan.

Appendix A.1: Reaction, Diffusion and Convection Model

Chemical pattern dynamics of the BZ reaction is usually described by the Oregonator model, which is derived from the reaction kinetics of the Field-Körös-Noyes (FKN) mechanism (VIDAL and HANUSSE, 1986; WINFREE, 1987; KAPRAL and SHOWALTER, 1995). WILKE (1995), VASQUEZ *et al.* (1993) and WU *et al.* (1995) proposed the models of the reaction-diffusion equations with the advection terms. The advection terms connects the Keener-Tyson version (KEENER and TYSON, 1986) of two-variable Oregonator model with the Navier-Stokes equation (VASQUEZ *et al.*, 1993; WILKE, 1995; WU *et al.*, 1995; MATTHIESSEN *et al.*, 1996). A set of equations is given as

$$\frac{\partial u}{\partial t}+\left(V_x\frac{\partial u}{\partial x}+V_y\frac{\partial u}{\partial y}\right)=D_u\nabla^2 u+\frac{1}{\varepsilon}\left(u(1-u)-fw\frac{u-q}{u+q}\right), \tag{A.1}$$

$$\frac{\partial w}{\partial t}+\left(V_x\frac{\partial w}{\partial x}+V_y\frac{\partial w}{\partial y}\right)=D_w\nabla^2 w+u-w, \tag{A.2}$$

where the variables u and w represent the dimensionless concentrations of two chemical species of activator ([$HBrO_2$]) and inhibitor ([$Fe(phen)_3]^{3+}$), respectively, the symbol ∇^2 represents the Laplacian, D_u and D_w are molecular diffusivities of u and w, and f, q and ε are constants related to the chemical kinetics. Here, we consider the two-dimensional case: cartesian coordinates are horizontal axis of x and vertical axis of y. The direction of gravity is parallel to the y-axis. The velocity components V_x and V_y are connected with the pressure p through the Navier-Stokes equations:

$$\frac{\partial V_x}{\partial t}+\left(V_x\frac{\partial V_x}{\partial x}+V_y\frac{\partial V_x}{\partial y}\right)=-\frac{1}{\rho_0}\frac{\partial P}{\partial x}+\nu\nabla^2 V_x, \tag{A.3}$$

$$\frac{\partial V_y}{\partial t}+\left(V_x\frac{\partial V_y}{\partial x}+V_y\frac{\partial V_y}{\partial y}\right)=\frac{\rho-\rho_0}{\rho_0}g-\frac{1}{\rho_0}\frac{\partial P}{\partial y}+\nu\nabla^2 V_y, \tag{A.4}$$

and

$$\frac{\partial V_x}{\partial x}+\frac{\partial V_y}{\partial y}=0. \tag{A.5}$$

Here, ν is the kinematic viscosity, g is the gravitational acceleration, and ρ is the density. Equation (A.5) assumes incompressible fluids. The parameter P is the reduced pressure and is related to the conventional pressure p as

$$P = p - \rho_0 g y. \tag{A.6}$$

This formulation assumes a linear dependence of density on the chemical concentrations as

$$\rho = \rho_0(1 - \beta_u(u - u_s) - \beta_w(w - w_s)). \tag{A.7}$$

Here, ρ_0 is the density of the bulk. The parameters β_u and β_w are the coefficients of linear expansion due to compositional change of u and w (POJMAN and EPSTEIN, 1990; POJMAN *et al.*, 1991a, b; WU *et al.*, 1995).

Appendix A.2: Marangoni Convection

Concentration differences of u and w and a temperature difference bring surface tension effects. The effects are represented by the surface boundary condition (the equilibrium of tangential stress) in numerical simulation as

$$\mu\frac{\partial V_x}{\partial y}=\sum_i \xi_i\frac{\partial c_i}{\partial x}+\zeta\frac{\partial T}{\partial x} \tag{A.8}$$

where $\xi_i = \partial\sigma/\partial c_i$, $\zeta = \partial\sigma/\partial T$, $c_1 = u$ and $c_2 = w$. Here, $\mu = \rho\gamma$ is the dynamic viscosity, and σ is the surface tension. The parameters ξ_i and ζ are related to the solutal Marangoni number M_{s_i} and the thermal Marangoni number M_a, respectively, represented as

$$M_{s_i} = \frac{\xi_i \delta c_i d}{\rho_0 D_i \nu} \tag{A.9}$$

$$M_a = -\frac{\xi_i \delta T d}{\rho_0 \kappa \nu} \tag{A.10}$$

where κ is the thermal diffusion coefficient. Temperature differences δT and concentration differences δc_i influence the surface tension (MÜLLER *et al.*, 1985a):

$$\sigma = \sigma_0 + \frac{\partial\sigma}{\partial T}\delta T + \sum_i \frac{\partial\sigma}{\partial c_i}\delta c_i = \sigma_0 + \zeta\delta T + \sum_i \xi_i \delta c_i \tag{A.11}$$

where σ_0 is a reference value at a temperature T_0 and chemical composition c_0.

REFERENCES

AGLADZE, K. I., KRINSKY, V. I. and PERTSOV, A. M. (1984) Chaos in the Non-Stirred Belousov-Zhabotinsky Reaction is induced by interaction of waves and sationary dissipative structures, *Nature*, **308**, 834–835.

BÖCKMANN, M., HESS, B. and MÜLLER, S. C. (1996) Temperature gradients traveling with chemical waves, *Phys. Rev. E*, **53**, No. 3, 5498–5501.

BORCKMANS, P. and DEWEL, G. (1988) Chemical structures and convection, in *Chemical to Biological Organization* (eds. M. Markus, S. C. Müller and G. Nicolis), pp. 114–121, Springer Series in Synagetics, 39, Springer, Berlin.

CASTERS, V., DULOS, E., BOISSONADE, J. and DE KEPPER, P. (1990) Experimental evidence of a standing turing-type nonequilibrium chemical pattern, *Phys. Rev. Lett.*, **64**, 2953–2956.

DE KEPPER, P., CASTERS, V. and BOISSONADE, J. (1991) Turing-type chemical patterns in the chlorite-iodide-malonic acid reaction, *Physica D*, **49**, 161–169.

DIEWALD, M. and BRAND, H. R. (1993) Chemically driven convection. A simple model, *Chem. Phys. Lett.*, **216**, No. 3, 4, 5, 6, 566–570.

DIEWALD, M. and BRAND, H. R. (1995) Chemically driven convection can stabilize turing patterns, *Phys. Rev. E*, **51**, No. 6, R5200–R5203.

DIEWALD, M., MATTHIESSEN, K., MÜLLER, S. C. and BRAND, H. R. (1996) Oscillatory hydrodynamic flow due to concentration dependence of surface tension, *Phys. Rev. Lett.*, **77**, No. 21, 4466–4469.

FIELD, R. J. and BURGER, M. (1985) *Oscillations and Traveling Waves in Chemical Systems*, Wiley, NY.

INOMOTO, O., ABE, K., YAMAGUCHI, T. and KAI, S. (2000) Bromomalonic acid induces transition from trigger wave to big wave in Belousov-Zhabotinsky Reaction, *Phys. Rev. E*, **61**, No. 5, 5326–5329.

ITO, H. (1994) Mescopic modeling of wave propagation in excitable media, *Physica D*, **79**, 16–40.

JAHNKE, W. and WINFREE, A. T. (1991) A survey of spiral-wave behaviors in the oregonator model, *Int. J. Bifurcation and Chaos*, **1**, 445–466.

KAI, S. and MIIKE, H. (1994) Hydrochemical soliton due to thermocapillary instability in Belousov-Zhabotinsky Reaction, *Physica A*, **204**, 346–358.

KAI, S., ARIYOSHI, T., INENAGA, S. and MIIKE, H. (1995) Curious properties of soliton induced by Marangoni instability in shallow Belousov-Zhabotinsky Reaction, *Physica D*, **84**, 269–275.

KAPRAL, R. and SHOWALTER, K. (1995) *Chemical Waves and Patterns*, Kluwer Academic Publisher, Dordrecht/Boston/London.

KEENER, J. P. and TYSON, J. J. (1986) Spiral waves in the Belousov-Zhabotinskii Reaction, *Physica D*, **21D**, 307–324.

KSHIRSAFER, G., NOSZTICZIUS, Z., MCCORMICK, W. D. and SWINNEY, H. L. (1991) Spatial patterns in a uniformly fed membrane reactor, *Physica D*, **49**, 5–12.

LEE, K.-L., MCCORMICK, D., PEARSON, J. E. and SWINNEY, H. L. (1994) Experimental observation of self-replicative spots in a reaction-diffusion system, *Nature*, **369**, 215–218.

MATTHIESSEN, K. and MÜLLER, S. C. (1995) Global flow waves in chemically induced convection, *Phys. Rev. E*, **52**, No. 1, 492–495.

MATTHIESSEN, K., WILKE, H. and MÜLLER, S. C. (1996) Influence of surface tension changes on hydrodynamic flow induced by traveling chemical waves, *Phys. Rev. E*, **53**, 6056–6060.

MIIKE, H. and MÜLLER, S. C. (1993) Tubulent decomposition of chemical waves by spontaneously induced hydrodynamic oscillation, *CHAOS*, **3**, No. 1, 21–25.

MIIKE, H., MÜLLER, S. C. and HESS, B. (1988a) Oscillatory hydrodynamic flow induced by chemical waves, *Chem. Phys. Lett*., **144**, 515–520.

MIIKE, H., MÜLLER, S. C. and HESS, B. (1988b) Oscillatory deformation of chemical waves induced by surface flow, *Phys. Rev. Lett*., **61**, No. 18, 2109–2112.

MIIKE, H., MÜLLER, S. C. and HESS, B. (1989) Hydrodynamic flows traveling with chemical waves, *Phys. Lett*., **141**, No. 1, 2, 25–30.

MIIKE, H., YAMAMOTO, H., MOMOTA, M. and HASHIMOTO, H. (1992) in *Pattern Formation in Complex Dissipative Systems* (ed. S. Kai), pp. 191–200, World Scientific, Singapore.

MIIKE, H., YAMAMOTO H., KAI, S. and MÜLLER, S. C. (1993) Accelerating chemical waves accompanied by traveling hydrodynamic motion and surface deformation, *Phys. Rev. E*, **48**, No. 3, 627–1630.

MIIKE, H., SAKURAI, T., OSA, A. and YOKOYAMA, E. (1997) Observation of brownian motion by microscope image sequence processing, *J. Phys. Soc. Japan*, **166**, 1647–1655.

MIKHAILOV, A. S., DAVYDOV, V. A. and ZYKOV, V. S. (1994) Complex dynamics of spiral waves and motion of curves, *Physica D*, **70**, 1–39.

MÜLLER, S. C. and MIIKE, H. (1990) Pattern dynamics by interaction of chemical waves and hydrodynamic flows, in *New Trends in Nonlinear Dynamics and Pattern-Forming Phenomena* (eds. P. Coullet and P. Huerre), pp. 11–19, Plenum Press, NY.

MÜLLER, S. C., PLESSER, Th. and HESS, B. (1985a) Surface tension driven convection in chemical and biological solution layers, *Bur. Bunsenges. Phys. Chem*., **89**, 654–658.

MÜLLER, S. C., PLESSER, Th. and HESS, B. (1985b) Two-dimensional spectrophotometry with high spatial and temporal resolution by digital video techniques and powerful computers, *Analytical Biochemistry*, **146**, 125–133.

MÜLLER, S. C., PLESSER, Th. and HESS, B. (1987) Distinctive sites in chemical waves: The spiral core and the collision area of two annuli, *J. Statistical Phys*., **48**, No. 5, 6, 991–1004.

MÜLLER, S. C., PLESSER, Th. and HESS, B. (1989) Chemical waves and natural convection, in *Physicochemical Hydrodynamics: Interfacial Phenomena* (ed. M. G. Velarde), pp. 423–433, Plenum, NY.

NOSZTICZIUS, Z., HORSTHEMKE, W., MCCORMICK, W. D., SWINNEY, H. L. and TAM, W. Y. (1987) Sustained chemical waves in an annual gel reactor: A chemical pinwheel, *Nature*, **329**, 619–620.

ORBAN, M. (1980) Stationary and moving structures in uncatalyzed oscillatory chemical reactions, *J. Am. Chem. Soc*., **102**, 4311–4314.

PEARSON, J. E. (1993) Complex patterns in a simple system, *Science*, **261**, 189–192.

PLESSER, Th., WILKE, H. and Winters, K. H. (1992) Interaction of chemical waves with convective flows induced by density gradients, *Chem. Phys. Lett*., **200**, No. 1, 2, 158–162.

POJMAN, J. A. and EPSTEIN, I. R. (1990) Convective effects on chemical waves. 1. Mechanisms and stability criteria, *J. Phys. Chem*., **94**, 4966–4972.

POJMAN, J. A., EPSTEIN, I. R., MCMANUS, T. J. and SHOWALTER, K. (1991a) Convective effects on chemical waves. 2. Simple convection in the iodate-arsenous acid system, *J. Phys. Chem*., **95**, 1299–1306.

POJMAN, J. A., NAGY, I. P. and EPSTEIN, I. R. (1991b) Convective effects on chemical waves. 3. Multicomponent convection in the Iron(II)-Nitric acid system, *J. Phys. Chem*., **95**, 1306–1311.

SAKURAI, T., YOKOYAMA, E. and MIIKE, H. (1997a) Propagation of surface deformation coupled with convection waves under the excitation of a chemical wave train, *Phys. Rev. E*, **56**, No. 3, R2367–R2370.

SAKURAI, T., MIIKE, H., YOKOYAMA, E. and MÜLLER, S. C. (1997b) Initiation front and annihilation center of convection waves developing in spiral structures of Belousov-Zhabotinsky Reaction, *J. Phys. Soc. Japan*, **66**, No. 3, 518–521.

SAKURAI, T., MIIKE, H., OKADA, K. and MÜLLER, S. C. (2003) Spiral flow wave in a reaction-diffusion-convection system, *J. Phys. Soc. Japan* (in press).

SCHWABE, D., MOLLER, U., SCHNEIDER, J. and SCHARMANN, A. (1992) Instability of shallow dynamic thermocapillary liquid layers, *Phys. Fluids A*, **4**, 2368–2381.

TAM, W. Y., HORSTHEMKE, W., NOSZTICZIUS, Z. and SWINNEY, H. L. (1988) Sustained spiral waves in a continuously fed unstirred chemical reactor, *J. Chem. Phys.*, **388**, 3395–3396.

TURING, A. M. (1952) The chemical basis of morphgenesis, philosophical transactions of the Royal Society of London, Ser. B, *Biological Science*, **237**, 37–72.

VASQUEZ, D. A., WILDER, J. W. and EDWARDS, B. E. (1993) Hydrodynamic instability of chemical waves, *J. Chem. Phys.*, **98**, No. 3, 2138–2143.

VIDAL, C. and HANUSSE, P. (1986) Non-equilibrium behavior in isothermal liquid chemical systems, *Int. Rev. Phys. Chem.*, **5**, No. 1, 1–55.

WILKE, H. (1995) Interaction of traveling chemical waves with density driven hydrodynamic flows, *Physica D*, **86**, 508–513.

WINFREE, A. T. (1987) *When Time Breaks Down—The Three-Dimensional Dynamics of Electrochemical Waves and Cardiac Arrhythmias*, Princeton University Press, Princeton/New Jersey.

WU, Y., VASQUEZ, A., EDWARDS, E. and WILDER, W. (1995) Convective chemical-wave propagation in the Belousov-Zhabotinsky Reaction, *Phys. Rev. E*, **51**, No. 2, 1119–1127.

YOSHIKAWA, K., KUSUMI, T., UKITSU, M. and NAKATA, S. (1993) Generation of periodic force with oscillating chemical reaction, *Chem. Phys. Lett.*, **211**, 211–213.